ARTICLE

OBC
www.rsc.org/obc

Controlling conformations and physical properties of *meso*-tetrakis(phenylethynyl)porphyrins by ring fusion: synthesis, properties and structural characterizations

Zhen Shen,†[a] Hidemitsu Uno,*[b] Yusuke Shimizu[a] and Noboru Ono*[a]

[a] *Department of Chemistry, Faculty of Science, Ehime University, 2-5 Bunkyo-cho, Matsuyama, 790-8577, Japan. E-mail: ononbr@dpc.ehime-u.ac.jp; Fax: +81 899279590; Tel: +81 899279610*

[b] *Division of Synthesis and Analysis, Department of Molecular Science, Integrated Center for Sciences, Ehime University, 2-5 Bunkyo-cho, Matsuyama, 790-8577, Japan. E-mail: uno@dpc.ehime-u.ac.jp; Fax: +81 899279670; Tel: +81 899279660*

Received 17th August 2004, Accepted 30th September 2004
First published as an Advance Article on the web 5th November 2004

The boron trifluoride-catalyzed Rothemund condensations of phenylpropargylaldehyde with 4,7-dihydro-4,7-ethano-2*H*-isoindole or 3,4-diethylpyrrole in dichloromethane at low temperature give 5,10,15,20-tetrakis(phenylethynyl)porphyrins bearing bicyclo[2.2.2]octadiene and octaethyl substituents, respectively. The former undergoes a retro Diels–Alder reaction to afford 5,10,15,20-tetrakis(phenylethynyl)benzoporphyrin quantitatively. The different conformations of the porphyrin periphery were determined by X-ray diffraction and their redox and spectroscopic properties have been investigated.

Introduction

Porphyrinoids with high-wavelength absorptions have been extensively investigated in recent years due to their potential value as photosensitizers in photodynamic therapy (PDT),[1] but also as novel optical materials such as fluorescent probes and near-infrared dyes, and as components of photosynthetic antenna arrays.[2] Several approaches for the construction of red-shifted porphyrinoid systems have been reported, including the introduction of *meso*-alkynyl substituents,[3] the expansion of porphyrin chromophores,[4] porphyrin linkage isomerizations[5] and core modification.[6] The steric crowding of the peripheral substituents can cause conformational distortions of porphyrin rings and also results in the red-shift.[7] Recent investigations on porphyrins with fused aromatic subunits showed that such ring expansion produced minor bathochromic shifts to the Soret absorption except for acenaphthylene fusion.[8] On the other hand, arylethynyl *meso*-subsituents were found to red-shift the porphyrin B and Q bands significantly more than aryl *meso*-substituents, which is due to the efficient electron communication between porphyrin and aryl π-systems provided by the ethynyl group. We have previously reported a convenient synthetic route to prepare benzoporphyrins *via* retro Diels–Alder reaction from the bicyclo[2.2.2]octenediene (BCOD) ring-fused porphyrins.[9] To further extend the conjugation of the porphyrin core, we present here the first synthesis and structure characterization of *meso*-tetrakis(phenylethynyl)benzoporphyrin.

Results and discussion

Synthesis of *meso*-tetrakis(phenylethynyl)porphyrins

Recently, H. L. Anderson and co-workers have reported that the boron trifluoride-catalyzed reaction of acetylenic aldehydes with 3,4-diethylpyrrole generated various *meso*-alkynyl porphyrinoids with contracted and expanded structures.[10] Since the unsubstituted isoindole is too unstable to be used directly for the preparation of related benzoporphyrins, it occurred to us to apply the 4,7-dihydro-4,7-ethano-2*H*-isoindole as its precursor for porphyrin synthesis.[9a] As shown in Scheme 1, the synthesis of *meso*-substituted porphyrins was adapted according to the procedure developed by Anderson and co-workers. 3,4-Diethylpyrrole[11] and 4,7-dihydro-4,7-ethano-2*H*-isoindole[9b] were prepared according to the published procedures. 4,7-Dihydro-4,7-ethano-2*H*-isoindole condensed with phenylpropynal in dry dichloromethane at −40 °C using $BF_3{\cdot}OEt_2$ as catalyst, followed by oxidation with 2,3-dichloro-5,6-dicyano-1,4-benzoquinone (DDQ) produced BCOD ring-fused *meso*-tetrakis(phenylethynyl)porphyrin H_2-**1** in 10% yield. Heating H_2-**1** at 230 °C *in vacuo* for 30 min give pure *meso*-tetrakis(phenylethynyl)benzoporphyrin H_2-**2** quantitatively. The *meso*-tetrakis(phenylethynyl)octaethylporphyrin H_2-**3** was prepared as a main product in 20% yield from 3,4-diethylpyrrole using a similar method.

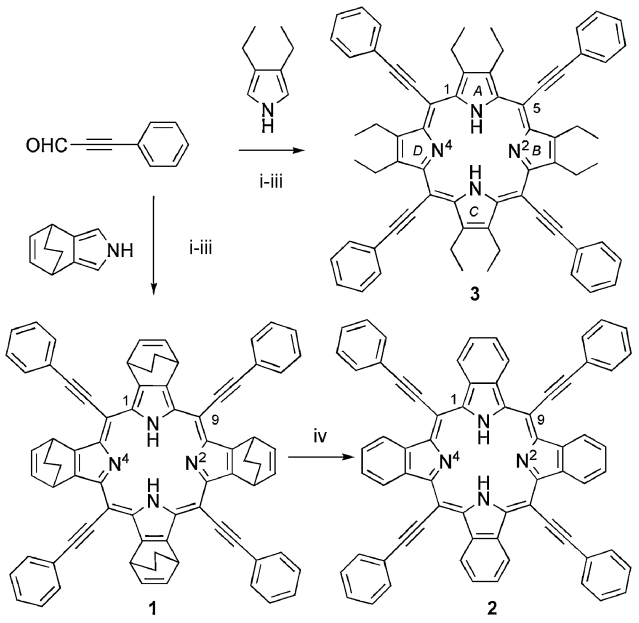

Scheme 1 *Reagents and conditions*: i, $BF_3{\cdot}OEt_2$; ii, DDQ; iii, Et_3N; iv, 230 °C, 30 min.

† Present address: State Key Laboratory of Coordination Chemistry, Nanjing University, Nanjing 210093, China.

DOI: 10.1039/b412688b

X-Ray analysis of porphyrins

Single crystals for X-ray analysis were obtained by slow evaporation of a mixed solution of $CHCl_3$ and MeOH for Zn-**1** and H_2-**3**, or $CHCl_3$ solution containing a small amount of pyridine for Zn-**2**. Their structures were subjected to X-ray analyses and the results are summarized in Table 1.[12] Radial views from the centre of the porphyrins are shown in Fig. 1. CCDC reference numbers 227105–227107. See http://www.rsc.org/suppdata/ob/b4/b412688b/ for crystallographic data in .cif format.

Porphyrin Zn-1. From the systematic absences, the space group was suggested to be *Cc* or *C*2/*c*. We solved and refined the structure in both *Cc* and *C*2/*c* space groups. In both cases, the structures were finally refined without methanol molecules by several cycles of SHELXL-97 and PLATON-SQUEEZE programs,[13] because even the coordinated methanol molecule was disordered. As the structure solved in *Cc* was unstable during the refinement, the phenyl and porphyrin ring atoms were tightly restrained and some atoms were treated isotropically. In the refined structure in *Cc*, the zinc atom showed out-of-plane disorder toward the coordinated methanol molecules with half occupancy. The final *R* values in the *Cc* space group were slightly better than those in the *C*2/*c* space group. The PLATON analysis, however, revealed a centre of symmetry in the structure of *Cc* space group with 100% fit. Thus, the centrosymmetric space group *C*2/*c* was chosen. The porphyrin macrocycle of Zn-**1** is slightly wave-structured with a mean plane deviation of 0.092 Å (Fig. 1a). The dihedral angles between the benzene rings and the porphyrin planes are 15.9(2)° and 34.8(2)° for the two types of aryl rings (Fig. 2). These values are much smaller than those for 5,10,15,20-tetra(4-*n*-butylphenylethynyl)porphyrin,[3a] indicating enhanced conjugation of the benzene plane and the porphyrin ring through the ethylene bridge.

Porphyrin Zn-2. The structure of Zn-**2**·C_5H_5N·$CHCl_3$, as shown in Fig. 1b, is ruffle-shaped with the maximum displacement of *meso*-pyrrole carbons from the mean plane of 0.480(3) Å. The isoindole units are almost flat (the mean deviations range from 0.015 to 0.036 Å). In this case, the zinc atom is coordinated to one pyridine molecule (in the positive region of Fig. 1) and displaced towards the pyridine ligand by 0.293(1) Å from the mean plane of four nitrogen atoms (Fig. 3). The dihedral angles

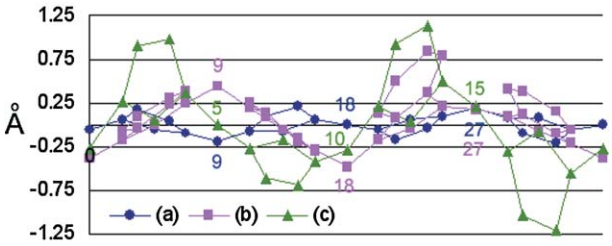

Fig. 1 Distortion diagram of the porphyrins. (a) Zn-**1**·2MeOH, −150 °C. (b) Zn-2·C_5H_5N·$CHCl_3$, −70 °C. (c) H_2-**3**, −70 °C. According to the numbering sequence, *meso*-positions are 9, 18, 27 and 36 in tetrabenzoporphyrin **2** and its precursor **1**, but 5, 10, 15 and 20 in porphyrin **3**.

of the benzene rings with the porphyrin planes are 23.4(1)°, 48.6(2)°, 53.3(3)° and 89.5(1)° respectively.

Porphyrin H_2-3. The free-base H_2-**3** adopts a heavily distorted saddle conformation with a maximum displacement of β-pyrrole carbons from the mean plane of 1.212(2) Å (Fig. 1c and Fig. 4). It is interesting to note that its crystal structure shows obvious in-plane nuclear reorganization (IPNR).[7] Localization of the inner hydrogen atom positions and bond characters was observed (Fig. 5): in comparison with H_2OETPP (2,3,7,8,12,13,17,18-octaethyl-5,10,15,20-tetraphenylporphyrin),[14] the *meso* and α-carbon bonds of C4–C5, C9–C10, C15–C16 and C20–C1 are elongated, with the average bond distance being 1.426 Å for H_2-**3**, while the bond lengths of C5–C6, C10–C11, C14–C15, C19–C20, N2–C9 and N4–C16 are shortened (the average bond distances of C···C and N···C for H_2-**3** are 1.403 and 1.347 Å, respectively). The tilting angles of pyrrole units to the mean porphyrin plane are A: 30.74(7)°, B: −24.27(6)°, C: 13.47(6)° and D: −27.78(6)°. This fact also supports the bond localization in this crystal structure. The acetylene groups almost lie within the mean planes of the benzene rings, while the dihedral angles of the benzene rings with the porphyrin planes are 18.7(1)°, 22.1(1)°, 34.0(1)° and 36.9(1)°, respectively.

The electronic absorption spectra are given in Fig. 6. The Soret bands of Zn-**1**, Zn-**2** and Zn-**3** are at 494, 528 and 508 nm, respectively, which are considerably red-shifted compared to those of *meso*-unsubstituted Zn-BCOD ring-fused porphyrin

Table 1 Crystallographic data for porphyrins[a]

Compound	Zn-**1**·2CH_3OH	Zn-**2**·C_5H_5N·$CHCl_3$	H_2-**3**
Formula	$C_{76}H_{52}N_4Zn$·2CH_3OH	$C_{68}H_{36}N_4Zn$·C_5H_5N· $CHCl_3$	$C_{68}H_{62}N_4$
FW	1150.74	1172.92	935.26
Temp./°C	−150	−70	−70
System	monoclinic	triclinic	triclinic
Space group	*C*2/*c*	$P\bar{1}$	$P\bar{1}$
a/Å	30.864(8)	12.6459(5)	10.785(2)
b/Å	11.647(2)	16.2904(10)	14.200(3)
c/Å	18.709(5)	16.4899(8)	17.438(4)
α/°	90	71.236(9)	94.857(4)
β/°	117.893(5)	63.449(8)	102.039(5)
γ/°	90	68.986(8)	90.567(4)
V/Å^3	5944(2)	2783.2(2)	2601.4(9)
Z	4	2	2
μ/cm^{-1}	0.467	0.637	0.069
$2\theta_{max}$/°	27.48	27.48	27.48
Unique reflns.	6725	12299	11556
No. obs.	3899	9795	7677
R_{int}	0.067	0.033	0.037
No. var.	371	760	708
R_1	0.102	0.059	0.070
wR(all)	0.321	0.180	0.199
Goodness of fit	1.072	1.002	1.001

[a] Mo-Kα was employed.

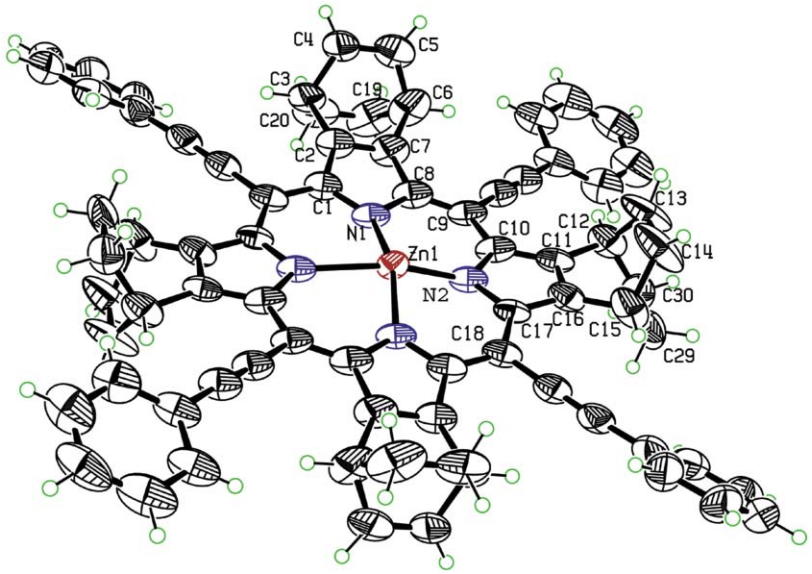

Fig. 2 ORTEP plot of the X-ray structure of Zn-**1** with thermal ellipsoids shown at 50%. By the PLATON SQUEEZE program, the structure was refined without methanol molecules.

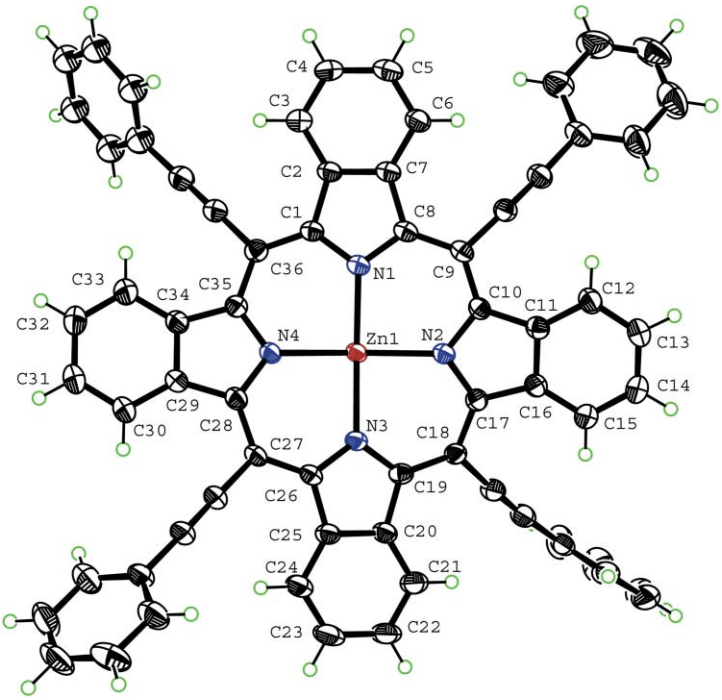

Fig. 3 ORTEP view of the X-ray structure of Zn-**2** with thermal ellipsoids shown at 50%. The disordered phenyl groups with lower occupancies, chloroform solvent and coordinated pyridine are omitted for clarity.

(400 nm), Zn-tetrabenzoporphyrin (425 nm in THF–pyridine) and ZnOEP (2,3,7,8,12,13,17,18-octaethylporphyrinato zinc) (403 nm). The Q bands of Zn-**1** (632 and 685 nm), Zn-**2** (676 and 737 nm) and Zn-**3** (653 and 714 nm) are also in the longer wavelength region than those of the Zn-BCOD porphyrin (534 and 561 nm), Zn-benzoporphyrin (622 nm) and ZnOEP (569 nm). The large bathochromic shift (around 100 nm) of the electronic absorptions of *meso*-(tetrakisphenylethynyl)porphyrins demonstrates that the phenylethynyl substituents considerably enhance the porphyrin conjugation. The absorption of Zn-**1** is blue-shifted compared to that of Zn-**3**. Since the electronic inductive properties of the ethyl and BCOD ring groups are thought to be similar, the difference should be primarily due to the conformational factor. The ^{1}H NMR chemical shift of NH in free base H_2-**1** appears at δ −1.72 ppm, whereas that of H_2-**3** appears at δ 0.26 ppm, indicating that H_2-**1** is more planar than H_2-**3** in solution. The red-shift of the spectrum of Zn-**2** compared to that of Zn-**1** is most likely due to the extended electronic conjugation by fused benzene rings.

The redox properties for Zn-**1**, Zn-**2** and Zn-**3** were studied by cyclic voltammetry (Table 2). Zn-**1** and Zn-**2** showed two reversible oxidation peaks, while Zn-**3** gave only one reversible peak. The first oxidation potentials of Zn-**1**, Zn-**2** and Zn-**3** were 0.34 V, 0.08 V and 0.25 V (*vs.* F_c/F_c^+), respectively. However, their first reduction potentials were similar, at −1.46 V for Zn-**1**, −1.47 V for Zn-**2** and −1.46 V for Zn-**3**. Zn-**2** was oxidized at a much lower potential than Zn-**1**, indicating that the HOMO energy level of Zn-**2** is considerably increased by fusion with benzene rings. Since the first reduction potential didn't change as much, the HOMO–LUMO separation in Zn-**2** is narrowed. This is in accordance with the red-shifts of the absorption bands of Zn-**2**. That Zn-**3** is more easily oxidized than Zn-**1**

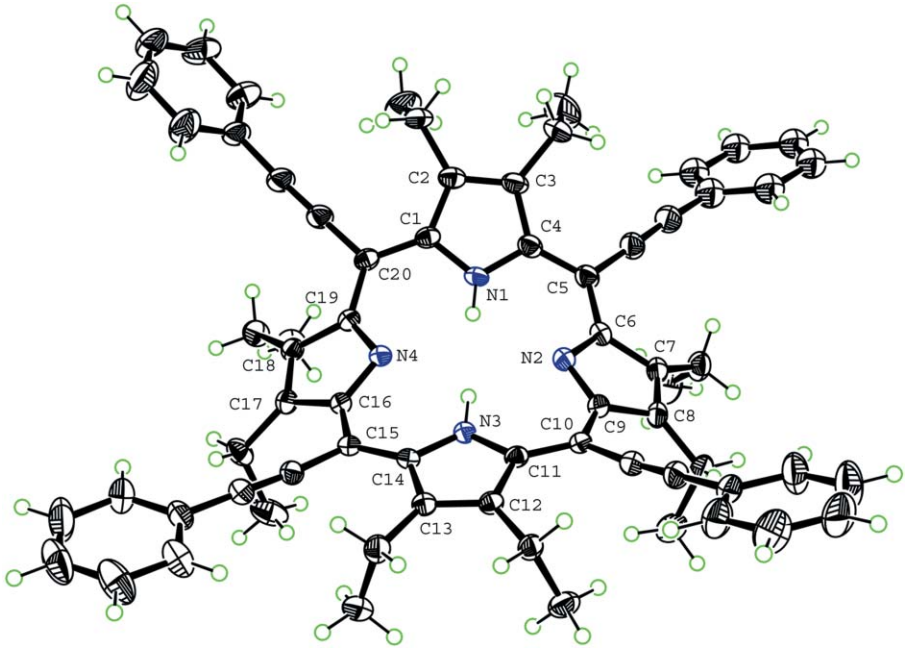

Fig. 4 ORTEP plot of H_2-**3** with thermal ellipsoids shown at 50%. Disordered ethyl and phenyl groups with lower occupancies are omitted for clarity.

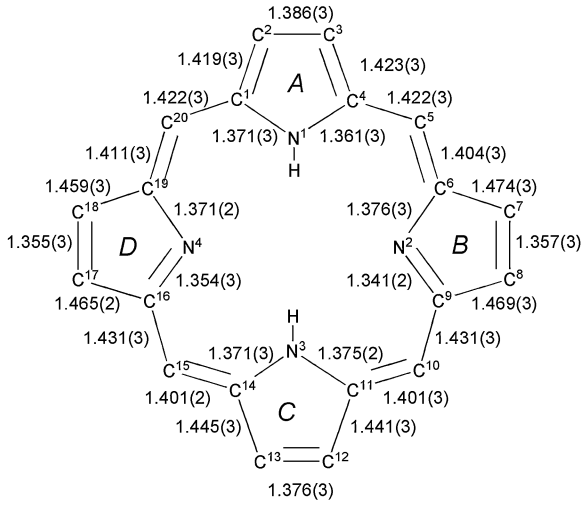

Fig. 5 Bond lengths of the H_2-**3** porphyrin core.

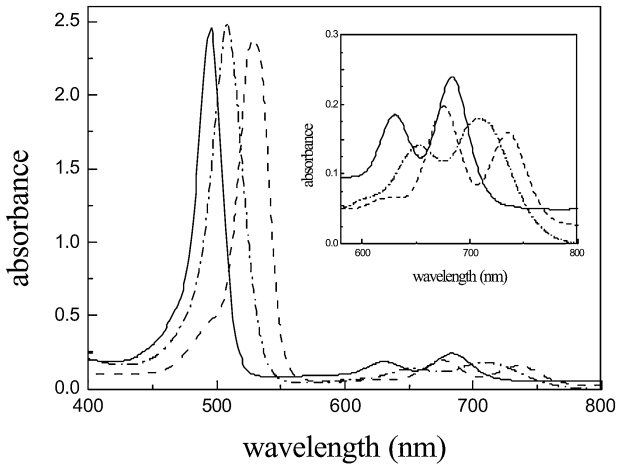

Fig. 6 UV-vis spectra of Zn-**1** (—), Zn-**2** (. . .) and Zn-**3** (---) in $CHCl_3$. Inset: absorption spectra of the Q-band region.

may result from the distortion of Zn-**3**, which destabilizes its HOMO energy level. This is consistent with the blue-shift of the Zn-**1** absorption bands compared to Zn-**3**. Conformational distortions and substituent properties can significantly affect the redox potentials and spectroscopic properties of the porphyrin macrocycle.

Table 2 Redox potentials of porphyrins Zn-**1**, Zn-**2** and Zn-**3**.[a]

Porphyrin	$E_{1/2}$(ox)/V	E_p(red)/V
Zn-**1**	0.34, 0.56	−1.46
Zn-**2**	0.08, 0.40	−1.47
Zn-**3**	0.25, 0.67[b]	−1.46

[a] In CH_2Cl_2, $c = 10^{-3}$ M, 0.1 M TBAP, $\upsilon = 100$ mV s^{-1}, referenced against Fc^+/Fc. [b] Irreversible peak

Conclusion

In summary, incorporation of *meso*-phenylethynyl substituents and fusion of benzene rings to the porphyrin chromophore considerably changes its redox potential and leads to large red-shifts in the electronic absorption spectra. The tetrabenzoporphyrins have not been well studied due to the difficulty of preparation and their poor solubility in most organic solvents, while BCOD ring-fused porphyrins are readily available by conventional and efficient porphyrin syntheses, and can be purified by recrystallization and/or chromatography. The bulky BCOD rings not only increase porphyrin solubility by preventing π–π stacking, but rigidify porphyrin rings to maintain the planar conformation. They are useful precursors for the construction of multi-tetrabenzoporphyrin arrays. In addition, we have found interesting bond localization of the porphyrin skeleton induced by the ring distortion in a crystalline state of porphyrin H_2-**3**.

Experimental

Melting points were measured with a Yanagimoto BY-1 melting point apparatus. Unless otherwise noted, ^{1}H NMR and ^{13}C NMR spectra were recorded in $CDCl_3$ solution on a JEOL EX 400 spectrometer at ambient temperature. NMR chemical shifts are expressed in ppm using TMS as an internal standard, and coupling constants were measured in Hz. UV-vis spectra were obtained with Shimadzu UV-2200 spectrometers. Mass spectra were measured with a JEOL JMS-700 spectrometer (70 eV for EI and *m*-nitrobenzyl alcohol as the matrix for FAB). Elemental analysis was performed with a Yanako MT-5 recorder.

Cyclic voltammograms were obtained in CH_2Cl_2–0.1 M TBAP (tetra-*n*-butylammonium perchlorate) on a BAS electrochemical analyzer model BS-1, using a platinum disk as the working electrode, $Ag/AgNO_3$ as the quasi-reference electrode, and a platinum wire as the counter electrode. Redox potentials were referenced internally against ferrocenium/ferrocene (Fc^+/Fc). Measurements were performed under inert atmosphere at room temperature with a scan rate of 100 mV s^{-1}. THF was distilled from sodium benzophenone ketyl and dichloromethane was distilled from CaH_2 prior to use. Pyridine was distilled from CaH_2 and stored over 4 Å MS. Deuterated solvents were used without further purification. 3,4-Diethylpyrrole[11] and 4,7-dihydro-4,7-ethano-2*H*-isoindole[9b] were prepared according to published procedures.

9,18,27,36-Tetrakis(phenylethynyl)-3,6,12,15,21,24,30,33-octahydro-3,6;12,15;21,24;30,33-tetraethano-37*H*,39*H*-tetrabenzoporphine (H_2-1)

Boron trifluoride etherate (120 μL, 0.99 mmol) was added to a stirred solution of phenylpropynal (430 mg, 3.3 mmol) and 4,7-dihydro-4,7-ethano-2*H*-isoindole (480 mg, 3.3 mmol) in 350 mL dry CH_2Cl_2 under N_2 at −40 °C. After stirring for 3 h at −40 °C in the dark, the mixture was allowed to warm up to room temperature overnight. DDQ (749 mg, 3.3 mmol) was added and the reaction mixture was stirred for an additional 1 h. 1 mL of triethylamine was added and the solvents removed *in vacuo*. The residue was purified by column chromatography on silica gel, eluting with 1% Et_3N–$CHCl_3$. The product was collected as a green fraction. Following evaporation of the solvents under reduced pressure, the residue was recrystallized from chloroform–methanol. The title compound was obtained in 10% yield as a mixture of diastereomers. Greenish crystals, mp 180 °C (decomposed). δ_H −1.72 (2H, s), 1.98–2.17 (16H, m), 6.4 (8H, m), 6.92–7.01 (8H, m), 7.54–7.66 (12H, m) and 8.03–8.05 (8H, m). MS (FAB), *m*/*z*: 1024 [MH^+]. Elemental analysis, calcd (%) for $C_{76}H_{54}N_4 \cdot 2H_2O$: C, 86.17; H, 5.52; N, 5.29. Found: C, 86.46; H, 5.29; N, 5.15. UV-vis, λ_{max} ($CHCl_3$)/nm (ε/dm^3 mol^{-1} cm^{-1}): 494 (2.47×10^5), 632 (1.86×10^4) and 685 (2.44×10^4).

5,10,15,20-Tetrakis(phenylethynyl)-2,3,7,8,12,13,17,18-octaethyl-21*H*,23*H*-porphine (H_2-3)

$BF_3 \cdot OEt_2$ (160 μL) was added to a solution of 3,4-diethylpyrrole (492 mg, 4 mmol) and phenylpropynal (521 mg, 4mmol) in 400 mL dry CH_2Cl_2 under N_2 at −40 °C. After stirring for 3 h at −40 °C in the dark, the mixture was allowed to warm up to room temperature overnight. DDQ (908 mg, 4 mmol) was added followed by triethylamine (1 mL). The reaction mixture was purified by column chromatography and recrystallization from chloroform–methanol. Yield: 200 mg, 20%. Greenish crystals, mp >250 °C. δ_H 0.26 (2H, s), 1.49 (24H, t, J = 7.3 Hz), 3.94 (16H, q, J = 7.3 Hz), 7.45–7.53 (12H, m) and 7.78–7.80 (8H, m). δ_C 16.70, 20.66, 91.02, 98.66, 105.04, 124.19, 128.54, 128.71, 130.92, 143.39 and 143.94. MS (FAB) *m*/*z*: 936 [MH^+]. Elemental analysis, calcd (%) for $C_{68}H_{62}N_4 \cdot H_2O$: C, 85.68; H, 6.77; N, 5.87. Found: C, 85.57; H, 6.57; N, 5.72. UV-vis, λ_{max} ($CHCl_3$)/nm (ε/dm^3 mol^{-1} cm^{-1}): 502 (1.68×10^5), 607 (1.09×10^4), 666 (2.39×10^4) and 778 (8×10^3).

9,18,27,36-Tetrakis(phenylethynyl)-3,6,12,15,21,24,30,33-octahydro-3,6;12,15;21,24;30,33-tetraethanotetrabenzoporphyrinato zinc (Zn-1):

$Zn(OAc)_2 \cdot 2H_2O$ (100 mg, 0.46 mmol) in MeOH (3 mL) was added to H_2-**1** (40 mg, 0.039 mmol) in $CHCl_3$ (10 mL). The mixture was stirred for 3 h at room temperature. The solution was washed with water (40 mL) and brine (20 mL), and dried over anhydrous Na_2SO_4. After evaporation, the product was purified by recrystallization from $CHCl_3$–MeOH to give Zn-**1** (38 mg, 90%) as greenish needles: mp 180 °C (decomposed). δ_H 2.12–2.17 (16H, m), 6.58 (8H, m), 6.96–7.11 (8H, m), 7.51–7.65 (12H, m), 8.04–8.06 (8H, m). MS (FAB) *m*/*z*: 1086 [M^+]. Elemental analysis, calcd (%) for $C_{76}H_{52}N_4Zn \cdot 1.5H_2O$: C, 81.97; H, 4.98; N, 5.03. Found: C, 81.71; H, 4.89; N, 4.79. UV-vis, λ_{max} ($CHCl_3$)/nm (ε/dm^3 mol^{-1} cm^{-1}): 494 (2.47×10^5), 631 (1.97×10^4) and 685 (2.50×10^4).

5,10,15,20-Tetrakis(phenylethynyl)-2,3,7,8,12,13,17,18-octaethylporphyrinato zinc (Zn-3)

The title compound was prepared in quantitative yield by a method similar to that described above. Greenish crystals, mp >250 °C. δ_H 1.52 (24H, t, J = 7.3 Hz), 4.01 (16H, q, J = 7.3 Hz), 7.47–7.55 (12H, m) and 7.81–7.83 (8H, m). MS (FAB) *m*/*z*: 998 [M^+]. Elemental analysis, calcd (%) for $C_{68}H_{60}N_4Zn$: C, 81.79; H, 6.06; N, 5.61. Found: C, 81.56; H, 6.01; N, 5.53. UV-vis, λ_{max} ($CHCl_3$)/nm (ε/dm^3 mol^{-1} cm^{-1}): 508 (2.49×10^5), 652 (1.61×10^4) and 714 (1.97×10^4).

9,18,27,36-Tetrakis(phenylethynyl)tetrabenzoporphyrinato zinc (Zn-2)

Zn-**1** (20 mg, 0.018 mmol) was heated in a sample tube under vacuum (10 mmHg) at 230 °C for 30 min to give Zn-**2**. Yield 18 mg, 100% without purification. Green powder, mp >250 °C. δ_H (C_5D_5N) 7.48–7.52 (4H, m), 7.60–7.64 (8H, m), 8.07–8.09 (8H, m), 8.18–8.2 (8H, m) and 10.63–10.65 (8H, m). δ_C (C_5D_5N) 95.7, 97.6, 104.3, 124.5, 125.6, 127.7, 129.2, 129.6, 131.8, 139.1 and 144.6. MS (FAB) *m*/*z*: 973 [M^+]. Elemental analysis, calcd (%) for $C_{68}H_{36}N_4Zn \cdot 1.5H_2O$: C, 81.55; H, 3.93; N, 5.59. Found: C, 81.39; H, 3.84; N, 5.51. UV-vis, λ_{max} ($CHCl_3$)/nm (ε/dm^3 mol^{-1} cm^{-1}): 528 (2.39×10^5), 676 (2.05×10^4) and 737 (1.65×10^4).

Acknowledgements

This work was partially supported by Grants-in-Aid for Scientific Research from the Ministry of Education, Culture, Sports, Science and Technology of Japan and by JSPS postdoctoral fellowship (to Z.S.). We thank the Research Center for Molecular-Scale Nanoscience (IMS) for carrying out X-ray measurements (AFC7R-Mercury CCD).

References

1 (*a*) S. B. Brown and T. G. Truscott, *Chem. Br.*, 1993, **29**, 955; (*b*) D. Dolphin, *Can. J. Chem.*, 1994, **72**, 1005; (*c*) R. Bonnett, *Chem. Soc. Rev.*, 1995, **24**, 19.
2 S. Prathapan, T. E. Johnson and J. S. Lindsey, *J. Am. Chem. Soc.*, 1994, **115**, 7519.
3 (*a*) H. L. Anderson, A. P. Wylie and K. Prout, *J. Chem. Soc., Perkin Trans. 1*, 1998, 1607, and references therein; (*b*) H. L. Anderson, *Chem. Commun.*, 1999, 2323; (*c*) P. N. Taylor, A. P. Wylie, J. Huuskonen and H. L. Anderson, *Angew. Chem., Int. Ed.*, 1998, **37**, 986; (*d*) S. M. Kuebler, R. G. Denning and H. L. Anderson, *J. Am. Chem. Soc.*, 2000, **122**, 339; (*e*) T. E. O. Screen, K. B. Lawton, G. S. Wilson, N. Dolney, R. Ispasoiu, T. Goodson, S. J. Martin, D. D. C. Bradley and H. L. Anderson, *J. Mater. Chem.*, 2001, **11**, 312.
4 (*a*) J. L. Sessler and A. K. Burrell, *Top. Curr. Chem.*, 1991, **161**, 177; (*b*) B. Franck and A. Nonn, *Angew. Chem., Int. Ed. Engl.*, 1995, **34**, 1795.
5 (*a*) E. Vogel, M. Kocher, H. Schmickler and J. Lex, *Angew. Chem., Int. Ed. Engl.*, 1986, **25**, 257; (*b*) P. J. Chmielewski, L. Latos-Grazynski, K. Rachlewcz and T. Glowiak, *Angew. Chem., Int. Ed. Engl.*, 1994, **33**, 779; (*c*) H. Furuta, T. Asano and T. Ogawa, *J. Am. Chem. Soc.*, 1994, **116**, 767.
6 (*a*) M. J. Broadhurst, R. Grigg and A. W. Johnson, *J. Chem. Soc. C*, 1971, 3681; (*b*) E. Vogel, W. Haas, B. Knipp, J. Lex and H. Schmickler, *Angew. Chem., Int. Ed. Engl.*, 1988, **27**, 406; (*c*) T. D. Lash, *Angew. Chem., Int. Ed. Engl.*, 1995, **34**, 2533.
7 R. E. Haddad, S. Gazeau, J. Pecaut, J. Marchon, C. J. Medforth and J. A. Shelnutt, *J. Am. Chem. Soc.*, 2003, **125**, 1253, and references therein.

8 (*a*) T. D. Lash, *J. Porphyrins Phthalocyanines*, 2001, **5**, 267; (*b*) T. D. Lash, *Energy Fuels*, 1993, **7**, 166, and references therein; (*c*) T. D. Lash and P. Chandrasekar, *J. Am. Chem. Soc.*, 1996, **118**, 8767.
9 (*a*) S. Ito, T. Murashima and N. Ono, *J. Chem. Soc., Perkin Trans. 1*, 1997, 3161; (*b*) S. Ito, T. Murashima, H. Uno and N. Ono, *Chem. Commun.*, 1998, 1661; (*c*) S. Ito, N. Ochi, T. Murashima, H. Uno and N. Ono, *Heterocycles*, 2000, **52**, 399.
10 A. Krivokapic, A. R. Cowley and H. L. Anderson, *J. Org. Chem.*, 2003, **68**, 1089.
11 L. Sessler, A. Mozaffari and M. R. Johnson, *Org. Synth.*, 1998, **9**, 242.
12 X-Ray data were processed by CrystalStructure Version 3.6.0 (Rigaku, 3–9-12 Akishima, Tokyo, Japan). Structures were solved by SIR-97 and then refined by CRYSTALS and/or SHELXL-97. When the PLATON SQUEEZE program was applied, the data cited in the text refer to the structures refined by several cycles of SHELXL-97 and PLATON SQUEEZE programs.
13 A. L. Spek, *PLATON, A Multipurpose Crystallographic Tool*, 2003, Utrecht University, Utrecht, The Netherlands; A. L. Spek, *J. Appl. Cryst.*, 2003, **36**, 7.
14 A. Regev, T. Galili, C. J. Medforth, K. M. Smith, K. M. Barkigia, J. Fajer and H. Levanon, *J. Phys. Chem.*, 1994, **98**, 2520.